DRAFT SF 298

1. Report Date (dd-mm-yy)	2. Report Type	3. Dates covered (from... to)
4. Title & subtitle Nonequilibrium Alloying of Aluminum for Improving the Corrosion Resistance of Graphite-Reinforced Metal matrix Composites Tri-Service Committee on Corrosion Proceedings		5a. Contract or Grant # 5b. Program Element #
6. Author(s) Dr. Barbara A. Shaw, Ms Tia R. Schrecengost, Mr Paul L. Miller, Mr. Robert G. Wendt, Dr. William C. Moshier		5c. Project # 5d. Task # 5e. Work Unit #
7. Performing Organization Name & Address		8. Performing Organization Report #
9. Sponsoring/Monitoring Agency Name & Address Tri-Service Committee on Corrosion USAF WRIGHT-PATTERSON Air Force Base, Ohio 45433		10. Monitor Acronym 11. Monitor Report #
12. Distribution/Availability Statement Approved for Public Release Distribution Unlimited		
13. Supplementary Notes		
14. Abstract		
15. Subject Terms Tri-Service Conference on Corrosion		

Security Classification of			19. Limitation of Abstract	20. # of Pages	21. Responsible Person (Name and Telephone #)
16. Report	17. Abstract	18. This Page			

TRI-SERVICE CONFERENCE ON CORROSION

21-23 JUNE 1994

SHERATON PLAZA HOTEL
ORLANDO, FLORIDA

PROCEEDINGS

Nonequilibrium Alloying of Aluminum for Improving the Corrosion Resistance of Graphite-Reinforced Metal Matrix Composites

Dr. Barbara A. Shaw,* Ms.Tia R. Schrecengost, Mr. Paul L. Miller
The Pennsylvania State University, University Park, PA 16802

Mr. Robert G. Wendt and Dr. William C. Moshier
Martin Marietta Astronautics Group, Denver, CO 80201

INTRODUCTION

High modulus graphite (Gr) reinforced metal matrix composites (MMCs) offer a wide variety of attractive properties including: high specific modulus and strength (E/ρ and UTS/ρ), tailorable or zero coefficient of thermal expansion (CTE), and high thermal conductivity. Using Al as the matrix metal results in a reduction of the final density of the composite with high elastic modulus and excellent strength in the fiber direction. Unfortunately, MMCs, especially Gr reinforced composites, are extremely susceptible to corrosion with severe attack in chloride-containing environments occurring in as little time as several weeks for Gr/Al composites.[1-3]

The overall objective of this research is to determine whether improving the inherent passivity of the matrix metal in a Gr/Al composite can alleviate, or at least minimize, galvanic corrosion between the graphite and the matrix metal. This galvanic corrosion is currently the limiting factor in utilization of these composites. Our research focuses on the unique properties of sputter deposited alloys. With sputter deposition it is possible to significantly increase the solubility of passivity enhancing species, thus dramatically improving their corrosion resistance.[4-8] The approach being undertaken is to develop alloy systems capable of minimizing galvanic degradation of the composite. An essential step in this process is identification of alloy compositions which maintain enhanced passivity after processing into the bulk composite. Our earlier work[4,5,8] indicated that Al-Mo alloys provide the best combination of thermal stability, corrosion resistance, and alloy density. This paper will address the thermal stability and corrosion resistance of selected

compositions of Al-Mo and Al-Mg-Mo alloys. Once the best candidate is identified from these alloys, sputter-coated graphite fibers can be consolidated into a component, such as the mirror support structure for a staring telescope schematically illustrated in Figure 1.

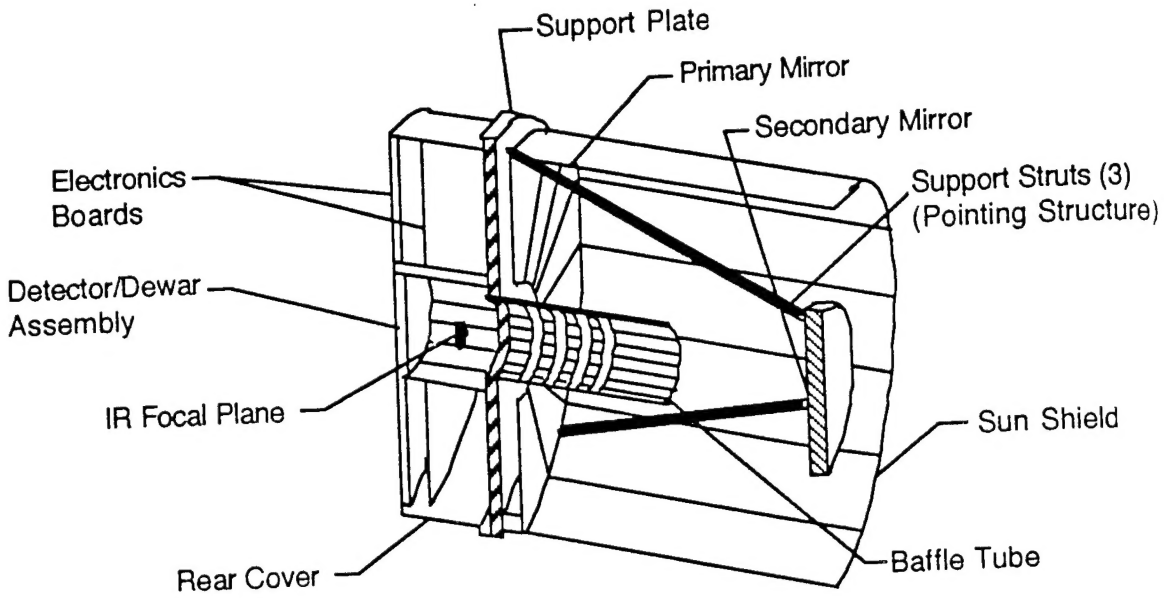

Figure 1. Schematic of a Staring Telescope.

EXPERIMENTAL

The alloys were fabricated by RF and DC magnetron sputter deposition using a 602RS Thin Film Deposition System. High purity targets were sputtered onto either sapphire or single crystal silicon wafers, yielding alloy films approximately 1 to 2 μm thick. Substrate temperature was not controlled during sputtering and reached a maximum temperature of approximately 100 °C during a 1 hour deposition. Pressure in the chamber was held constant at 7.0 mtorr during sputtering by introducing purified (< 10 ppb O_2) Ar gas at a flow rate of 200 standard cubic centimeters per minute (sccm) and adjusting the conductance of the system. Uniform alloy composition on each wafer was maintained by spacing the sputtering heads approximately 10 cm from the substrate, focused 60° from the substrate normal and rotating the substrate at 30 rpm during deposition.

Prior to electrochemical testing, x-ray diffraction (XRD), selected area diffraction (SAD) and transmission electron microscopy (TEM) were used to characterize the structure of the alloys and determine if the solute was maintained in solid solution with the base metal.

Alloy surfaces were characterized using optical microscopy, scanning electron microscopy (SEM), and scanning laser microscopy (SLM). Optical microscopy and SLM were used prior to electrochemical testing to observe surface defects such as scratches and cracks incorporated during sputtering and handling (i.e., cleaving of the alloy-coated Si wafer) of the alloy. SEM was also used prior to polarization so that EDS could be employed for semi-quantitative compositional analysis. All three microscopy techniques were used following electrochemical testing so that the morphology of the breakdown regions could be evaluated.

Test specimens were prepared by cleaving the alloy-coated Si wafer into pieces with areas of approximately 4 to 5 cm^2. Individual pieces were then coupled to a potentiostat through a lead wire and all regions, except the test area, were coated with an adherent marine epoxy to ensure that environmental and electrical isolation were maintained. Anodic and cathodic polarization experiments were performed using a conventional three electrode technique, consisting of a saturated calomel reference electrode (SCE), graphite counter electrodes, and sample electrode. The polarization behavior was used to assess passivation behavior in the alloys and for the construction of galvanic diagrams. These diagrams are useful in predicting the coupled current in a galvanic cell. Unless specifically noted, all potentials reported in this paper are referenced to a SCE. Polarization scans were generated at a scan rate of 0.2 mV/sec in 0.1 M NaCl solution adjusted to a pH of 8 with 0.1 M NaOH solution. The corrosion potential (E_{oc}) was allowed to stabilize in the test solution for approximately 60 minutes prior to polarization. A minimum of two tests were conducted for each condition to confirm the validity of results.

Electrochemical response of the graphite fibers was measured by testing an AMOCO composite consisting of 62.5 vol. % P75 Gr fibers embedded in ERXL 1962. Prior to testing, the edges of the specimens (with an approximate graphite area of 0.74 cm^2) were sanded to reveal the fibers and in order to make an electrical connection. The specimen was electrically isolated by embedding the AMOCO composite in an epoxide resin. The graphite was cathodically polarized at a scan rate equivalent to the anodic scans, and the area of the graphite was estimated by measuring the tested surface area and multiplying it by the fiber area fraction of the exposed surface (55 %) calculated with an image analyzer.

To confirm the galvanic diagram predictions, galvanic currents were measured by coupling either the as-sputtered or heat treated alloy specimens to P75 Gr fibers. The P75 Gr fibers were prepared for testing by embedding them into a non-conductive epoxy and electrically connecting them to a external lead. Area fractions of the exposed Gr

fibers were measured using a image analyzer. Nominal cathode-to-anode area ratios ranged from 0.2 to 1.1. The alloy specimen and the P75 Gr/epoxy composite were electrically coupled and immersed in a pH 8, 0.1 M NaCl solution. Galvanic current was monitored as a function of time using a potentiostat/zero resistance ammeter (operating in the ZRA mode).

RESULTS AND DISCUSSION

XRD revealed that all of the as-sputtered alloys were amorphous and contained no precipitates as shown in the representative pattern in Figure 2. Table 1 summarizes the XRD results of the alloys that were heat treated at 400°C, 500°C and 600°C for 1, 2, and 8 h to determine the effect of composite consolidation on the alloy structure. This table shows that as the concentration of Mo in the Al alloy increased, its propensity to form precipitates during heat treatment decreased. For example, Al-11Mo precipitated at the lowest time (1 h) and temperature (400°C); whereas, the Al-23Mo remained amorphous after being heat treated at 600°C for 2 h. This result was unexpected because as the Mo concentration increases, the thermodynamic driving force for precipitation increases. Lack of precipitation indicated the kinetics for precipitation in these alloys was very sluggish. The Al-Mg-Mo alloys were also amorphous in the as-sputtered condition, but were found to react at all heat treatment times and temperatures forming precipitates as well as oxides due to reaction of the Mg with the sapphire substrate.

TEM was conducted on the Al-18Mo in the as-sputtered condition and after heat treatment at 400°C for 2 and 8 h and 500°C for 2 and 8 hours. Figure 3 shows the representative structure of the as-sputtered alloy with the corresponding SAD pattern. Structure of the as-deposited Al-Mo alloy is featureless with the exception of the mottled appearance that resulted from the extensive ion milling used to thin the specimen. The SAD pattern shows two diffuse rings that correspond to the d-values calculated for the broad peaks found on the XRD patterns. Similar structures and SAD patterns were obtained for the Al-18Mo alloy heat treated at 400°C for 2 and 8 h which correlate with the XRD patterns that showed that the alloy remained amorphous after heat treatment. After heat treatment to 500°C for 2 and 8 h small precipitates began to appear (Figure 4). SAD of these precipitates indicate a structure of $Al_{12}Mo$, Al_5Mo, and Al. Not all the rings for each phase could be indexed and many of the rings could not be correlated with the expected Al-Mo intermetallic compounds. SAD of the Al-18Mo alloy heat treated at 500°C for 8 h shows an elongation of the diffraction spots which arises from fine precipitates that are preferentially oriented.

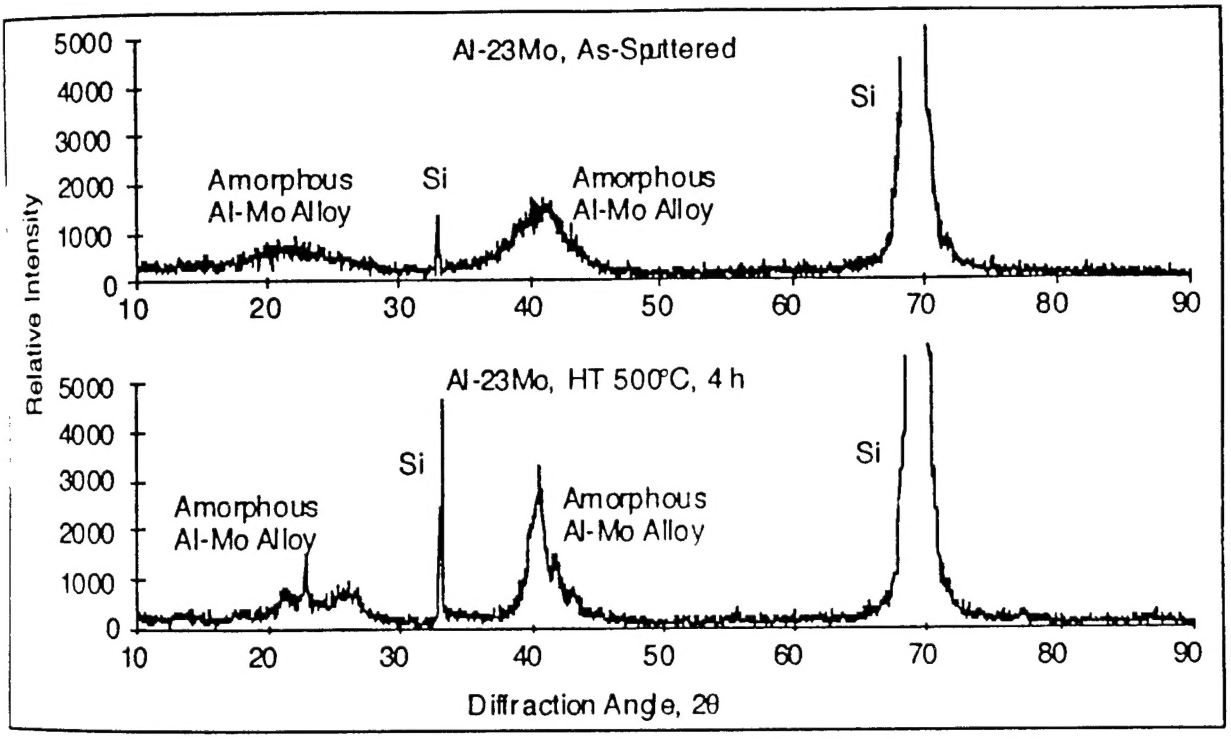

Figure 2. X-ray Diffraction of Al-23Mo in the As-Sputtered Condition and After Heat Treatment. As-Sputtered, the Alloy is Amorphous and it is Just Beginning to Precipitate after Heat Treatment at 500°C for 2 h.

Table 1. Summary of Al-Mo Alloy Structure as a Function of Heat Treatment Time and Temperature.

Heat Treatment Time (h)	Heat Treatment Temperature		
	400°C	500°C	600°C
1	Al-11Mo, ppt Al-18Mo, Amorphous Al-23Mo, Amorphous	Al-11Mo, ppt Al-18Mo, ppt Al-23Mo, Amorphous	Al-11Mo, ppt Al-18Mo, ppt Al-23Mo, Amorphous
2	Al-11Mo, ppt Al-18Mo, Amorphous Al-23Mo, Amorphous	Al-11Mo, ppt Al-18Mo, ppt Al-23Mo, Amorphous	Al-11Mo, ppt Al-18Mo, ppt Al-23Mo, Amorphous
8	Al-11Mo, ppt Al-18Mo, Amorphous Al-23Mo, Amorphous	Al-11Mo, ppt Al-18Mo, ppt Al-23Mo, Amorphous	Al-11Mo, ppt Al-18Mo, ppt Al-23Mo, ppt

ppt - fully precipitated

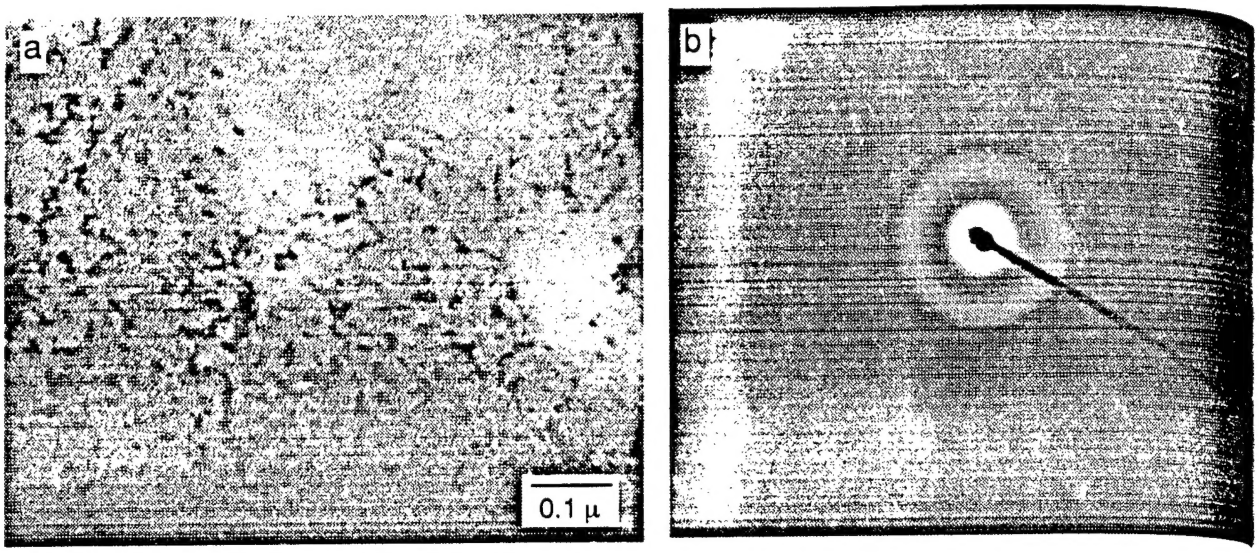

Figure 3. Structure and Associated SAD Pattern for the Amorphous Al-18Mo in the As-Deposited Condition and after Heat Treatment at 400°C for 2 and 8 h.

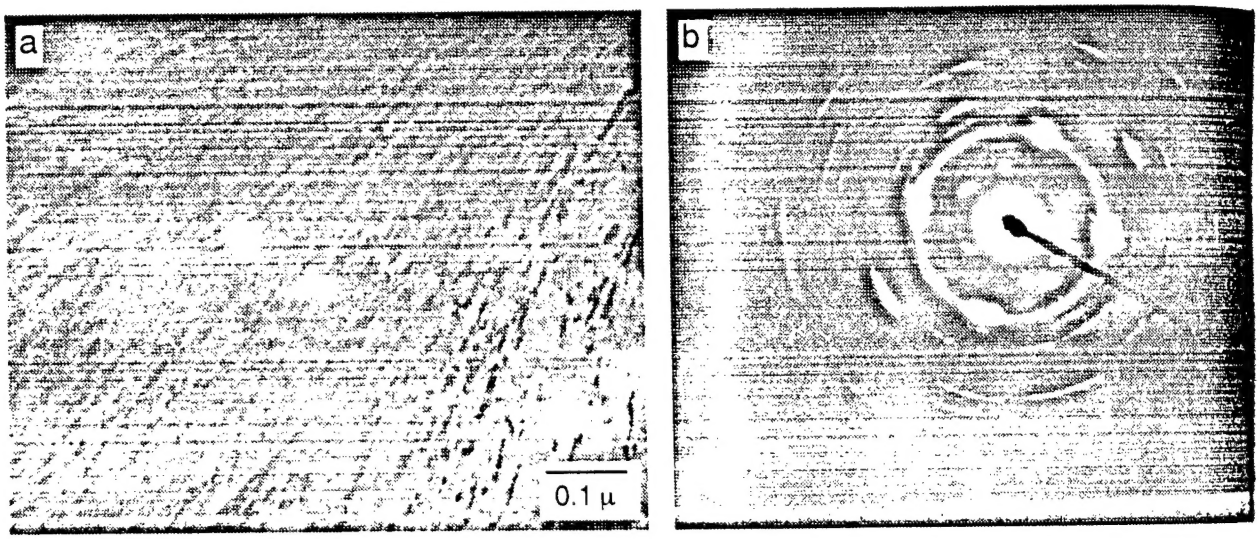

Figure 4. Structure (a) and SAD Pattern (b) for Al-18Mo, Heat-Treated at 500°C for 8 h. Fine Elongated Precipitates are Evident and the SAD Pattern Shows Elongated Spots that Correspond to the Fine Precipitate Structure.

Figure 5 summarizes the results of the anodic polarization experiments for the binary Al-Mo and ternary Al-Mg-Mo nonequilibrium alloys in the as-sputtered condition. All of the as-deposited Al-Mo alloys exhibited an extended passive region and an open circuit potential that was 500 to 600 mV more noble than pure Al. E_{oc} values for all of the alloys were measured to be between -600 to -450 mV_{SCE} with the majority of the measured E_{oc} values ranging from -520 mV_{SCE} to -580 mV_{SCE}. There was no apparent trend in E_{oc} as a function of solute concentration for the Al-Mo alloys tested, agreeing with the previous work on Al-Mo alloys.[9-11] Passive current densities (i_{pass}) for the as-deposited binary Al-Mo and ternary Al-Mg-Mo alloys ranged between 0.1 and 1.0 $\mu A/cm^2$, but as in the case of E_{oc}, no correlation between solute concentration and i_{pass} was evident. Variations in i_{pass} were attributed to general defects, i.e., scratches, pinholes, etc., in the alloy film. Breakdown potential (E_b) values for most of the as sputtered alloys were between 100 and 500 mV_{SCE} as compared to -690 mV_{SCE} for pure Al.

The polarization response of as-deposited and heat treated Al-11Mo alloys is shown in Figure 6. Although E_b for the heat treated Al-11Mo alloys decreased from ~420 mV_{SCE} (as-sputtered) to 50 mV_{SCE}, (heat treated), E_{oc} remained relatively constant at approximately -550 mV_{SCE}. Reduction in E_b was likely the result of precipitates formed during heat treatment creating microgalvanic cells with the surrounding alloy. Conversely, i_{pass} decreased from ~1 $\mu A/cm^2$ for the as-deposited alloy to ~0.1 $\mu A/cm^2$ after heat treatment.

Both E_{oc} and E_b for the Al-18Mo alloy were not dramatically affected by heat treating up to 500°C for 2 h (Figure 7). Similar to the Al-11Mo alloys, i_{pass} for the heat treated Al-18Mo specimens was less than that for the as-sputtered alloy, with the exception of specimen heat treated at 400°C for 1 h. No cracks or defects which may contribute to lower E_b values were found during SEM examination of the heat treated alloys.

Heat treatment of the Al-12Mg-13Mo alloy resulted in a more active E_{oc} (approximately -800 mV_{SCE}) with no passive response during polarization with exception of heat treating at 400°C for 1 h where E_{oc} was maintained.

SEM examination and EDS analysis of a newly formed pit on the as-deposited Al-18Mo specimen immediately after polarization to the breakdown potential showed the Mo concentration had risen from 18 to 25 atomic percent in the pit. Increase in Mo in the forming pit indicates the pitting process involves the preferential dissolution of Al from the alloy, which is consistent with x-ray photoelectron spectroscopy work conducted during earlier studies.[10,11]

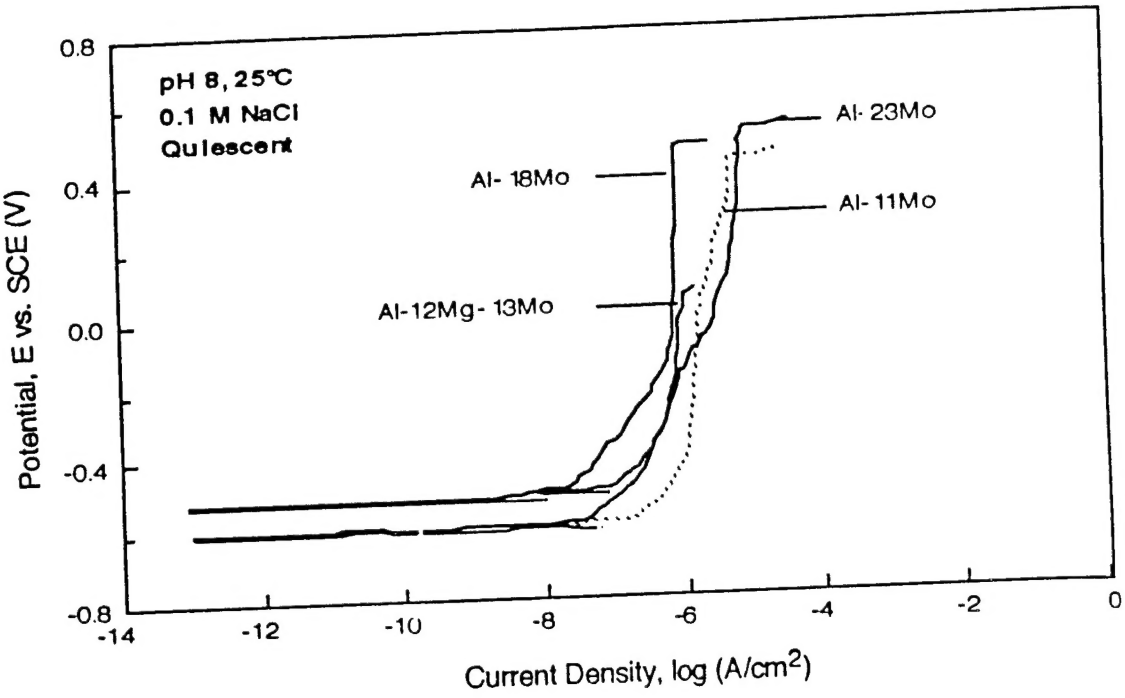

Figure 5. Anodic Polarization Response of Various Al-Mo Alloys, Polarized in 0.1M NaCl, pH 8, 25°C.

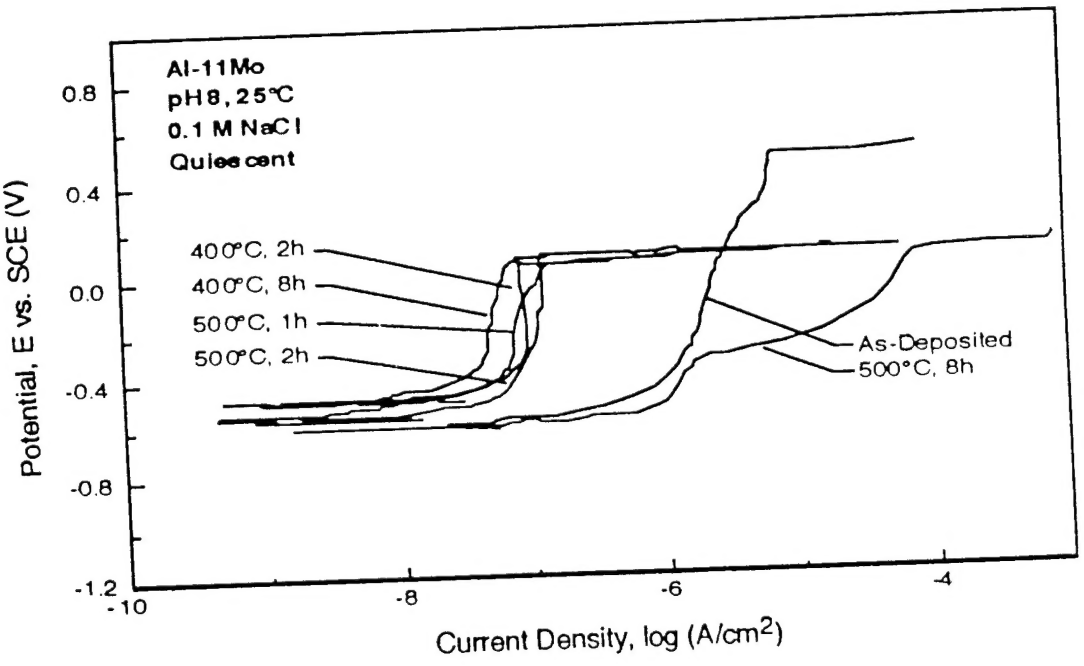

Figure 6. Anodic Polarization Response of Al-11Mo Before and After Heat Treatment at 400°C for 1 and 2 h and 500°C for 1, 2, and 8 h. Polarized in 0.1 M NaCl, pH 8, 25°C.

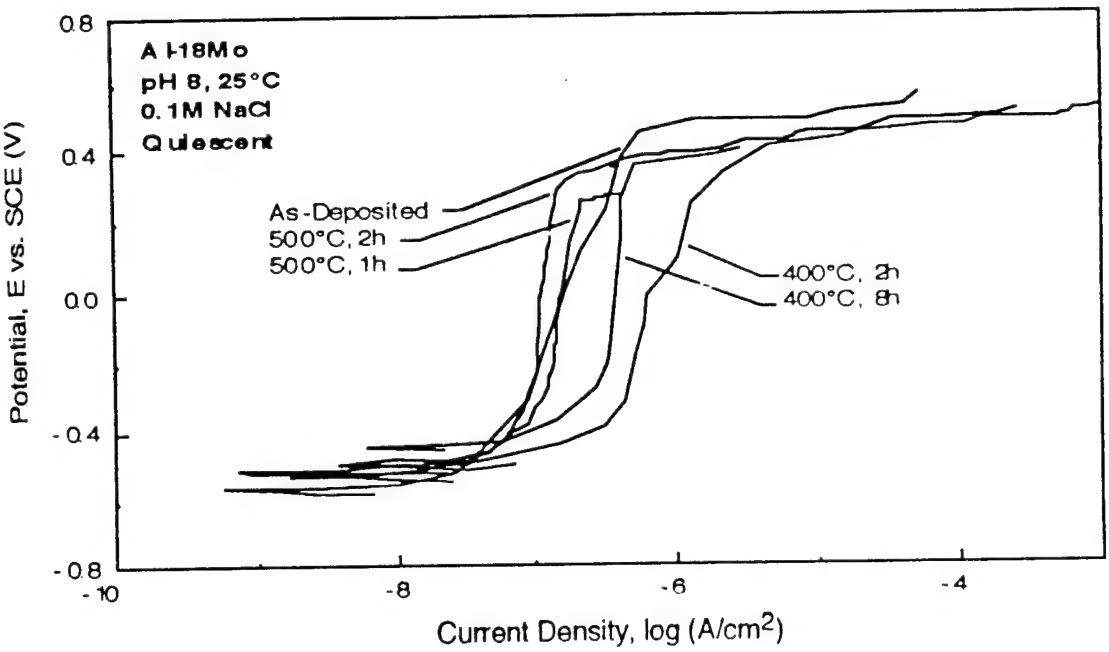

Figure 7. Anodic Polarization Response of Al-18Mo Before and After Heat Treatment at 400°C for 2 and 8 h and 500°C for 1 and 2 h, Polarized in 0.1 M NaCl, pH 8, 25°C.

The polarization data can be used to predict the current resulting in a galvanic couple. By superimposing the cathodic curve for graphite onto the anodic curves for the different sputtered alloys, the galvanic corrosion current can be estimated from the intersection of the two curves providing there is an insignificant IR drop, the contribution of other contributing reactions is small, and the current density is uniform.[12] Effects of the galvanic couple on the corrosion of the matrix metal can be easily estimated with such a diagram, and the diagrams can also be used to look at the effects of the cathode-to-anode area ratio and to determine if a reaction should be anodically or cathodically controlled. A galvanic diagram based on equal metal/Gr areas for pure Al, 6061 Al, and the Al-Mo alloys coupled to P75 Gr fibers is shown in Figure 8. This diagram estimates that the galvanic corrosion of pure sputtered and 6061 Al coupled to P75 Gr fibers are cathodically controlled with a relatively high current density value of 12.5 $\mu A/cm^2$. For a cathodically controlled reaction, the cathodic curve shifts to a higher current density as the Gr-to-Al area ratio increases, which accelerates the corrosion rate of the Al matrix. Converse to pure Al, galvanic corrosion was anodically controlled for the Al-Mo alloys with an estimated galvanic current density of 1 $\mu A/cm^2$ or less. For anodically controlled corrosion, changing the Gr-to-Al area ratio and subsequently shifting the cathodic curve to higher

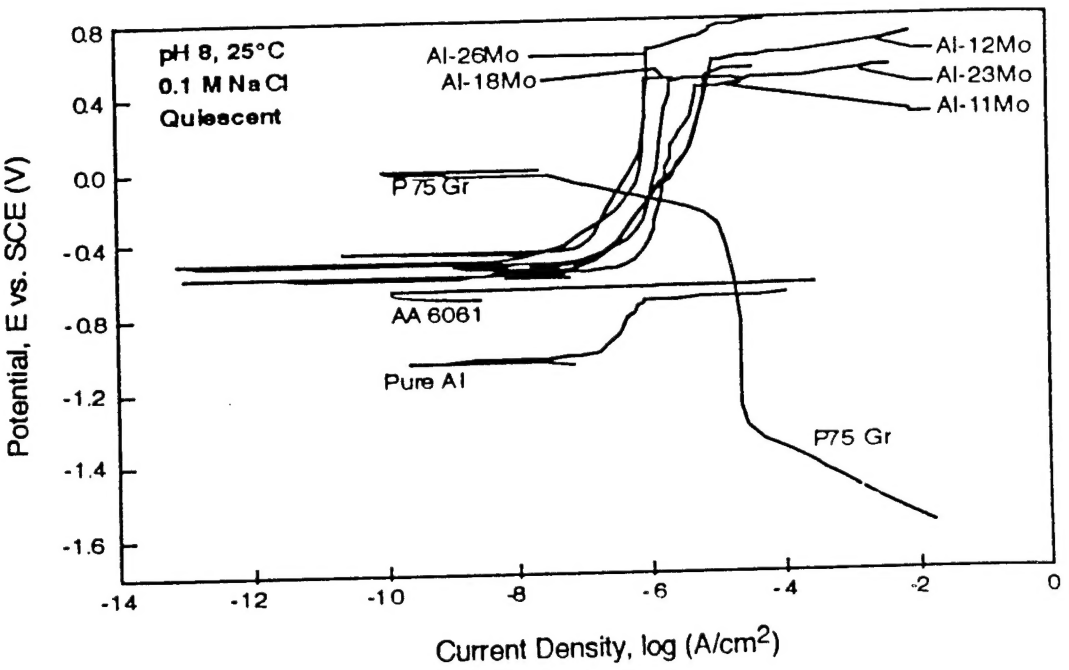

Figure 8. Galvanic Diagram with Anodic Curve of Pure Sputtered Aluminum, Wrought 6061 Al, and Various Sputtered Al-Mo Alloys Combined with the Cathodic Curve for an Equal Area of P75 Graphite Fibers, Tested in 0.1M NaCl, pH 8, 25°C.

current density values (or anodic curve to lower current density) would not significantly change the corrosion rate for the Al-Mo alloys. This result is important because modifying the Gr fiber volume, which is a key design feature of composites to achieve specific thermal or mechanical properties, will not result in dramatic changes in the corrosion response of the Gr/Al-Mo composite. The galvanic corrosion reaction remained anodically controlled for both the Al-11Mo and Al-18Mo alloys after heat treatment. Only after heat treating the Al-11Mo to 500°C for 8 h did control for the galvanic reaction change from anodic (Al passivation) to cathodic (oxygen reduction on Gr fibers).

To confirm the predictions made using the galvanic diagrams, long term galvanic current tests were conducted on sputtered Al, Al-11Mo, Al-18Mo, Al-23Mo, and ternary Al-12Mg-13Mo in the as-deposited condition by coupling the alloy to P75 Gr fibers (Figure 9). Galvanic current values are equivalent to current densities since the anode areas were 1 cm^2. For all the alloys, the galvanic current initially starts off at relatively high values between 3 and 30 $\mu A/cm^2$, but quickly drops to a low steady state value. The Al-18Mo and Al-23Mo reached low measured galvanic current densities of ~0.04 and ~0.08 $\mu A/cm^2$, respectively which were up to three orders of magnitude lower than the galvanic current density

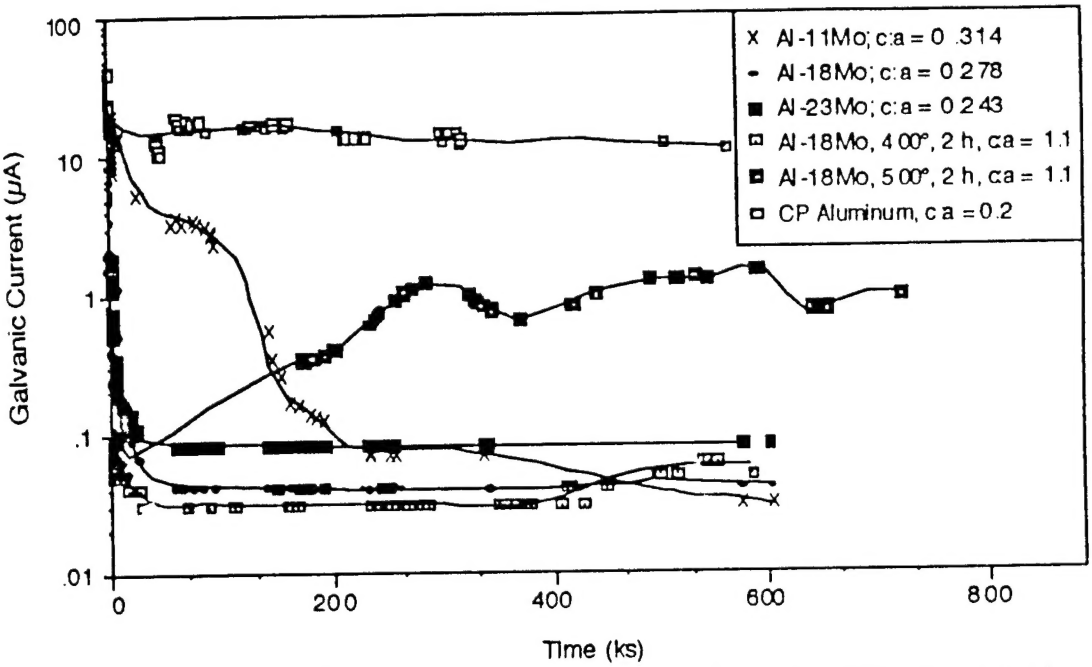

Figure 9. Galvanic Current for Commercially Pure Aluminum and Al-18Mo Alloys (As-Deposited and Heat Treated) Coupled to P75 Graphite Fibers in Quiescent 0.1M NaCl, pH 8, 25°C.

values of 30 $\mu A/cm^2$ measured for pure sputtered Al. The current density of the Al-18Mo after heat treatment at 400°C for 2 h was comparable to the as-sputtered value of 0.08 $\mu A/cm^2$. Even after heat treatment at 500°C for 2 h the galvanic current density was an order of magnitude lower than for pure sputtered Al. After galvanic testing for seven days (605 ks) the pure sputtered Al had completely dissolved from the Si wafer; whereas, the Al-Mo alloys remained intact and highly specular. The Al-12Mg-13Mo alloy exhibited a galvanic current value of 10 $\mu A/cm^2$ which is greater than the binary Al-Mo alloys but still 3 times lower than that of pure Al. However, less than 12 h (40 ks) after immersion in the 0.1 M NaCl, pH 8, solution, the Al-Mg-Mo alloys coupled to P75 Gr fibers exfoliated and completely lifted away from the substrate. Due to the short time in solution for the Al-12Mg-13Mo alloy, data for this alloys is not included in Figure 9.

Conclusions

Nonequilibrium Al-Mo alloys fabricated by magnetron sputtering have clearly been shown to be promising matrix alloys for Gr/Al composites. Al with 18 to 23 atomic percent Mo exhibited excellent corrosion resistance in the as-sputtered condition and could be heat treated up to 400°C for 8 h without detectable precipitation or change in

corrosion behavior. In addition, the Al-23Mo could be heat treated to 600°C for 2 h without degrading the corrosion performance. Galvanic current densities measured for Al-18Mo and Al-23Mo of ~0.04 to ~0.08 $\mu A/cm^2$ were 3 orders of magnitude lower than the 30 $\mu A/cm^2$ measured for pure Al in the 0.1 M NaCl, pH 8 solution when coupled to P75 Gr fibers. Galvanic diagrams of the anodic response of the alloy superimposed with the cathodic curve for the P75 Gr fibers predicted the galvanic corrosion rate to be controlled by the rate of the anodic reaction and the Al-Mo alloys were found to be electrochemically stable when coupled to Gr fibers regardless of the area ratios (in a 0.1M NaCl electrolyte). Based upon these results, an Al-Mo alloy with a Mo concentration of approximately 18 atomic percent was chosen to be deposited onto graphite fibers.

The ternary Al-12Mg-13Mo alloy is attractive because of its lower density. Unfortunately, this alloy exhibited a much higher galvanic current density value (~10 $\mu A/cm^2$) and was found to precipitate during heat treatment at the shortest time of 1 h and the lowest temperature of 400°C which resulted in a loss of passivation.

Acknowledgments

The authors gratefully acknowledge the support of A.J. Sedriks. This work was funded by the Office of Naval Research under contract N00014-91-J-1196.

References

1. D.M. Aylor and R.M. Kain, ASTM STP864 - Recent Advances in Composites in the US and Japan, Vinson and Taya (editors), American Society for Testing and Materials, Philadelphia, 632 (1985).
2. W.H. Pfeifer, W.J. Renton (editor), American Institute of Aeronautics and Astronautics, New York 231 (1977).
3. M.G. Vassilaros, D.A. Davis, G.L. Steckel, and J.P. Gudas, Proceedings of the 1980 Tri-Service Corrosion Conference, Vol. 2, US Government Publication, 21 (1980).
4. T.R. Schrecengost, M.S. Thesis, The Pennsylvania State University (1992).
5. R.G. Wendt, M.S. Thesis, Colorado School of Mines (1993)
6. P.L. Miller, M.S. Thesis, The Pennsylvania State University (1994).
7. P.L. Miller, B.A. Shaw, R.G. Wendt, and W.C. Moshier, "Technical Note: Improving Corrosion Resistance of Magnesium by Nonequilibrium Alloying with Yttrium," *Corrosion*, **49**, 947 (1993).

8. T.R. Schrecengost, B.A. Shaw, R.G. Wendt, and W.C. Moshier, "Nonequilibrium Alloying of Graphite-Reinforced Aluminum Metal Matrix Composites," *Corrosion*, **49**, 842 (1993).
9. W.C. Moshier, G.D. Davis, J.S. Ahearn, and H.F. Hough, "Influence of Molybdenum on the Pitting Corrosion of Aluminum Films," Journal of the Electrochemical Society, 1986, vol. 133, pp. 1063-1064.
10. W.C. Moshier, G.D. Davis, J.S. Ahearn, and H.F. Hough, "Corrosion Behavior of Aluminum-Molybdenum Alloys in Chloride Solutions," Journal of the Electrochemical Society, 1987, vol. 134, pp. 2677-2684.
11. G.D. Davis, W.C. Moshier, T.L. Fritz, and G.O. Cote, "Evolution of the Chemistry of Passive Films of Sputter-Deposited, Supersaturated Al Alloys," Journal of the Electrochemical Society, 1990, vol. 137, pp. 42[illegible].
12. D.A. Jones, Principles and Prevention of Corrosion, Macmillan Publishing Co., New York, 167 (1992).